




## A case study of bearing capacity of piles partially embedded in rock

Marília Dantas da Silva<sup>1#</sup> , Roberto Quental Coutinho<sup>1</sup> ,  
Bernadete Ragoni Danziger<sup>2</sup> 

Article

### Keywords

Bearing capacity  
Root piles  
Pile in rocks  
Dynamic tests on piles

### Abstract

In the design of piles partially embedded in rock, the main factors that influence the strength and deformability of the rock and the transmission of loads from pile to rock are of utmost relevance to pile behavior. Most empirical methods were developed based on data from specific regions. Differences in geological conditions, drilling methods and other features are not considered in most procedures. The article deals with a case of piles partially embedded in rock located in the town of São Lourenço da Mata, Pernambuco, Brazil. The rock mass consists of ancient deposits, formed mainly by granites of different compositions, gneiss and schists. The deposits have been deformed by several tectonic processes. Results from 99 dynamic loading tests enabled comparison between the mobilized lateral and pile toe resistance, with the estimated capacity obtained from the design methods known in the literature. In the prediction, the lateral shear resistance due to pile penetration in residual soil was also considered. Because failure was not reached in the dynamic tests, the estimated capacity was higher than the mobilized resistance. The resistances mobilized by the pile shaft friction in soil, by the pile shaft friction in rock and by the mobilized toe resistance in rock in the dynamic loading tests are compared to design methods known in the literature. Five static loading tests indicated failure loads greater than the mobilized resistance in the dynamic methods. The comparisons allow recommendations of the most consistent design methods to use in similar cases in practice.

## 1. Introduction

The bearing capacity of piles embedded in rock is difficult to predict. Few documented cases are available in the literature. This is the main reason for the lack of accuracy of the known design methods. Most methods present many uncertainties, leading to very conservative estimations. The lack of a more complete characterization of the rock and of an adequate number of tests are the reason for conservative design. The mobilized resistance in service conditions is usually many times lower than the available resistance.

Some authors, such as Rosenberg & Journeaux (1976), Horvath (1978) and Meigh & Wolski (1979) do not consider the toe resistance in rock when estimating the bearing capacity. Rowe & Armitage (1987) and Seidel & Collingwood (2001), consider that most of the working load is absorbed by the lateral resistance of the pile shaft in rock. Due to uncertainties regarding the proper cleaning of the base of the borehole and the concrete/rock interface behavior, toe resistance is

usually not considered in design. Toe resistance can only be considered if installation procedures ensure adequate cleaning of the bottom hole or when the load tests ensure mobilization of toe resistance (ABNT, 2019).

Empirical methods are based on data from specific regions and usually with a limited mechanical characterization of local rocks. Other aspects not considered, such as geological formations and differences in drilling methods, make empirical methods often unsuited for engineering applications. Few methods employ a rock quality index, such as the RQD, which considers rock mass discontinuities that influence shear strength (Xu et al., 2020).

This article analyzes a case study of a database consisting of 99 dynamic and 5 static tests on piles partially embedded in mainly granitic rock. The objective of the paper is to compare the mobilized resistance obtained in several dynamic loading tests and the conventional failure load in a small number of static loading tests to the capacity predicted by the design methods.

<sup>#</sup>Corresponding author. E-mail address: mariliadantas@hotmail.com

<sup>1</sup>Universidade Federal de Pernambuco, Grupo de Engenharia Geotécnica de Desastres e Planícies, Recife, PE, Brasil.

<sup>2</sup>Universidade Estadual do Rio de Janeiro, Instituto Alberto Luiz Coimbra de Pós-graduação e Pesquisa de Engenharia, Rio de Janeiro, RJ, Brasil.

Submitted on October 2, 2021; Final Acceptance on June 3, 2022; Discussion open until November 30, 2022.

<https://doi.org/10.28927/SR.2022.075521>



This is an Open Access article distributed under the terms of the Creative Commons Attribution License, which permits unrestricted use, distribution, and reproduction in any medium, provided the original work is properly cited.

The piles consisted of cast-in-place root piles excavated through soil and drilled in rock. A driving recoverable steel casing penetrated as far as the bedrock. From this level, the boring method involved compressed air assisted down-the-hole hammer drilling.

Dynamic tests were carried out according to NBR 13208 (ABNT, 2007). Pile resistance in soil/rock interface was obtained at blows with increasing energy. A pile driving analyzer (PDA) was used for data acquisition.

The dynamic test was analyzed by CAPWAP (Case Pile Wave Analysis Program) and some tests were also analyzed using the DINEXP program, in order to better investigate the mobilized resistance. Empirical methods available for piles partially embedded in rock were applied and compared to the test results.

The static loading tests were performed with a first slow maintained loading up to 1.2 times the service load (stabilized settlement criteria) followed by complete unloading. Second short-duration load increments (quick loading) were then proceeded up to twice the service load. The static loading tests gave some insight into the ratio conventional failure (extrapolated) bearing capacity to dynamic mobilized resistance.

The article discusses the main results and offers design suggestions.

## 2. Capacity estimation of piles partially embedded in rock

The load applied to the pile top is reduced along the shaft by the shear resistance on pile soil and pile rock contact surface. For heavy loads, part of the load is also transferred to the pile tip and the shear mobilized along the shaft may reach its residual value in part or throughout the whole length. Differences in this behavior are mainly due to rock features in the rock mass along the pile shaft. A proper rock characterization is then essential for ultimate capacity evaluation.

Lateral resistance results from the adhesion produced by the pile concrete at the hole's lateral interface, followed by shear at the pile-rock interface when initial adhesion is lost. Tip loading results from direct contact and transmission of the load from the pile to the rock (Goodman, 1989). Considering the three components of resistance (shear at pile soil interface, shear at pile rock contact and toe resistance), the toe resistance is commonly disregarded in piles embedded in rock due to the uncertainties regarding the clearance of the bottom hole (ABNT, 2019). Because pile displacement to reach peak lateral resistance in rock is much smaller than in soil, the lateral soil resistance is also disregarded in several methods. In the present article soil resistance was estimated by semi-empirical formulations used in Brazil (Aoki & Velloso, 1975; Décourt & Quaresma, 1978; Cabral, 1986).

The skin friction is usually estimated as a function of sleeve friction measured during the CPT tests. If CPT

tests are not available, the use of correlations established between the cone tip resistance with  $N_{60}$  from SPT can be used instead (Aoki & Velloso, 1975). Some other methods estimate pile soil lateral resistance directly from the  $N_{60}$  from SPT, according to Décourt & Quaresma (1978). Correction factors are necessary to consider installation procedures and scale effects. Aoki & Velloso (1975) consider the lateral soil resistance ( $Q_{l,s}$ ) given by Equation 1:

$$Q_{l,s} = U \sum \tau_{l,s} \Delta L \quad (1)$$

$U$  is the perimeter of the pile shaft,  $\tau_{l,s}$  is the shear soil resistance,  $\Delta L$  is the pile penetration in the soil layer.

Aoki & Velloso (1975) estimates soil resistance at the pile shaft using Equation 2:

$$\tau_{l,s} = \frac{\alpha k N_L}{F_2} \quad (2)$$

$k$  and  $\alpha$  are CPT x SPT correlation values depending on soil type,  $N_L$  is the average  $N_{60}$  value for a given soil layer with a  $\Delta L$  penetration and  $F_2$  is a factor expressing the installation and scale effects.

Décourt & Quaresma (1978) method, modified by Décourt (1996), suggests shear resistance using Equation 3:

$$\tau_{l,s} = (3.33\bar{N} + 10) \beta' \quad (kPa) \quad (3)$$

$\bar{N}$  is the average  $N_{60}$  value for the whole shaft penetration in soil, and  $\beta'$  is a coefficient given by Décourt (1996).

Cabral (1986) estimates the lateral resistance by Equation 4:

$$\tau_{l,s} = \beta_0 \beta_1 N_L \quad (kPa) \quad (4)$$

$\beta_0$ ,  $\beta_1$  are coefficients given by Cabral (1986) and  $N_L$  is the average  $N_{60}$  value for a given layer.

For the load capacity of piles embedded in rock, most authors correlate the lateral shear resistance ( $\tau_{l,r}$ ) and/or unit tip resistance ( $q_{p,r}$ ) with the uniaxial compressive strength of the intact rock ( $q_u$ ), given in Equation 5 and Equation 6.

$$\tau_{l,r} = \alpha q_u^\beta \quad (MPa) \quad (5)$$

$$q_{p,r} = N q_u^\rho \quad (MPa) \quad (6)$$

$\alpha$  and  $N$  are factors related to the quality of the rock mass and  $\beta$  and  $\rho$  are empirical parameters, Table 1.

The methods from AASHTO (1996), Cabral & Antunes (2000), España (2011) and Xu et al. (2020) proposed further considerations to estimate the bearing capacity of piles partially embedded in rock.

AASHTO (1996) does not consider the resistance contribution in soil. Toe resistance is considered only when the estimated settlement is greater than 1 cm. The total lateral and the toe resistance in rock are given by Equation 7 and Equation 8:

**Table 1.** Empirical coefficients for shear resistance in rock mass.

Reference	Shaft friction (MPa)
Rosenberg & Journeaux (1976)	$\tau_{m\acute{a}x} = 0.36(q_u)^{0.52}$
Horvath (1978)	$\tau_{m\acute{a}x} = 0.21(q_u)^{0.5}$
Meigh & Wolski (1979)	$\tau_{m\acute{a}x} = 0.22(q_u)^{0.6}$
Poulos & Davis (1980)	$\tau_{m\acute{a}x} = 0.05f_{cj}$ or $\tau_{m\acute{a}x} = 0.05q_u$
Rowe & Armitage (1987)	$\tau_{m\acute{a}x} = 0.45(q_u)^{0.5}$ or $\tau_{m\acute{a}x} = 0.6(q_u)^{0.5}$
Zhang & Einstein (1998)	$\tau_{m\acute{a}x} = 0.80(q_u)^{0.5}$ or $\tau_{m\acute{a}x} = 0.40(q_u)^{0.5}$

$f_{cj}$  is the uniaxial compressive strength of the concrete at de age of j days in MPa.

$$Q_{l,r} = \pi \phi_r L_r (0.144 \tau_{l,r}) \quad (7)$$

$$Q_{p,r} = N_{ms} q_u A_t \quad (8)$$

$\phi_r$  is the pile diameter in rock and  $L_r$  the pile length in rock,  $\tau_{l,r}$  is the shear resistance in rock,  $N_{ms}$  depends on rock type and quality,  $q_u$  is the uniaxial compressive strength of the intact rock and  $A_t$  is pile toe section.

The method by Cabral & Antunes (2000) considers the lateral friction contribution in soil. However, it is necessary that the soil provides adequate resistance and an elastic displacement greater than  $\delta_0$ , given in Equation 9.

$$\delta_0 = 2mm + 0.2\% \phi_s \quad (9)$$

$\phi_s$  is the pile diameter in soil.

The resistance at pile tip and the lateral shear of the pile embedded in rock are estimated by Equation 10 and Equation 11.

$$q_{p,r} = n \cdot q_u \leq 0.4 f_{ck} \quad (10)$$

$$\tau_{l,r} = 2.5 \text{ to } 3.5\% q_{p,r} < f_{ck} / 15 \quad (11)$$

$n$  is a correction factor that considers the rock alteration degree and the presence of small fractures in rock mass, as in Table 2 ( $f_{ck}$  is the concrete characteristic compressive strength).

The method proposed by España (2011) should not be applied to highly fractured rock ( $q_u < 1$  MPa) presenting an RQD  $< 10\%$  or to a highly weathered rock. For the tip resistance, España (2011) proposes an adaptation of the allowable stress of a shallow foundation in the same rock, increased by a factor of two.

España (2011) highlights that the allowable stress in shallow foundations depends on  $q_u$ , type of rock, degree of alteration and discontinuities spacing. The allowable stress is given by Equation 12.

**Table 2.**  $n$  values, Cabral & Antunes (2000).

Rock alteration degree	Variation Interval	Mean value
Highly weathered	0.07 - 0.13	0.1
Weathered	0.24 - 0.36	0.3
Moderately weathered to sound	0.48 - 0.60	0.54

$$P_{v,adm} = p_0 \alpha_1 \alpha_2 \alpha_3 \sqrt{\frac{q_u}{p_0}} \quad (MPa) \quad (12)$$

where  $\alpha_1$ ,  $\alpha_2$ ,  $\alpha_3$  are parameters depending on rock type, alteration degree and discontinuities spacing and  $p_0$  is the reference stress of 1 MPa. These parameters should represent the rock mass at a depth of  $1.5 \phi_r$  below toe.

The dimensionless parameters are estimated as follows:

The parameter  $\alpha_1$  can be determined in the laboratory, from specimens tested in traction, Equation 13:

$$\alpha_1 = \sqrt{\frac{10\sigma_t}{q_u}} \quad (13)$$

$\sigma_t$  is the rock tensile strength.

In case of no available tests, España (2011) recommends the values in Table 3.

In cases of a different rock at pile toe or doubts about classification,  $\alpha_1$  shall be 0.4.

For  $\alpha_2$ , the worst condition of the rock alteration degree found to a depth of  $1.5\phi_r$  from the tip must be considered. Values are shown in Table 4.

Regarding the influence of the discontinuity spacing ( $\alpha_3$ ), distinction between two forms of characterization must be identified: from the observation of the discontinuities emerging on an outcrop and from the RQD value.

For this analysis, the reference zone shall be the rock volume located below the foundation to a depth of  $1.5\phi_r$  and  $\alpha_3$  determined as the minimum value from the following relationships (Equation 14 and Equation 15):

$$\alpha_{3a} = \sqrt{\frac{S}{1m}} \quad (14)$$

$$\alpha_{3b} = \sqrt{\frac{RQD \%}{100}} \quad (15)$$

$S$  is the discontinuity spacings.

The toe resistance  $q_{p,r}$  obtained from the allowable  $P_{v,adm}$  is given by Equation 16.

$$q_{p,r} = 2P_{v,adm} \quad (MPa) \quad (16)$$

If the embedded length ( $L_r$ ) is significant and the rock mass has the same quality as that occurring under the tip, España (2011) proposes the application of an embedded factor to the tip resistance through Equation 17:

**Table 3.** Value of  $\alpha_1$ , España (2011).

Group	Designation	$\alpha_1$
1	Rock with well-developed structure	1
2	Igneous and metamorphic rocks*	0.8
3	Sedimentary** and some metamorphic rocks	0.64
4	Poorly consolidated rocks	0.4

(\*) Except rocks indicated in groups 1 and 3; (\*\*) Except rocks indicated in groups 1 and 4.

**Table 4.** Value of  $\alpha_2$ , España (2011).

Alteration degree	Designation	$\alpha_2$
I	Sound rock	1
II	Slightly weathered rock	0.7
III	Moderately weathered rock	0.5

$$d_f = 1 + 0.4 \frac{L_r}{\phi_r} \leq 2 \quad (17)$$

For the determination of shear strength in rock ( $\tau_{l,r}$ ), España (2011) suggests 10% of the tip resistance, Equation 18:

$$\tau_{l,r} = 0.1q_{p,r} \text{ (MPa)} \quad (18)$$

Xu et al. (2020) recommend Equation 19 and Equation 20 to predict shear resistance in rock, in MPa.

$$\tau_{l,r} = 0.532(\sigma_{cm3})^{0.425} \quad (19)$$

$$\sigma_{cm3} = q_u \cdot 10^{0.013RQD-1.34} \quad (20)$$

### 3. Back-analyses of the dynamic test

The force and velocity signals obtained in dynamic loading tests are usually analyzed with CAPWAP program, described by Goble et al. (1980). CAPWAP gives the resistance mobilized by the foundation soil in the instrumented blow.

The signals from CAPWAP were reprocessed with DINEXP, a similar program developed by Costa (1988). While CAPWAP is a commercial program, DINEXP routines are known in detail, Danziger (1991). This aspect enables a full understanding of signal matching by using DINEXP. As the uniqueness of CAPWAP results is questioned by some authors, the use of the two programs reduces possible uncertainties about the results (Danziger et al., 1996).

Costa (1988) applied the FEM in the formulation of DINEXP. The soil is represented by nonlinear springs with elastic-perfect plastic behavior, with dynamic resistance simulated by viscous elements (dash pots) with resistance directly proportional to particle velocity. The program was first conceived for application with the Smith (1960) model, alternative models known as Smith modified by Goble (1986) or Simons & Randolph (1985) can be adopted

instead. The time integration of the differential equilibrium equation system is made by the explicit central difference algorithm. The program includes a graphical routine that allows visualization of all calculated variables during the analysis for each node, particularly helpful to back-analysis purposes.

## 4. Case study

The case in study consists of the foundations of a football stadium covering an area of 130,000 m<sup>2</sup>. The stadium's "ring" structure occupies an extensive area. Significant variations in the stratigraphic profile are found. The soil and rock mass present layers of variable thicknesses associated with the geological-geotechnical model layout. The columns have service loads ranging from 1000 kN to 9000 kN, spanning 8-12 m. In part of the stadium the top of the rock mass is covered by alluvium, colluvium and/or residual soil. In other parts, there are rock outcrops.

### 4.1 Site characterization

The foundation consists of ancient deposits, mainly formed by granites of different compositions, gneiss and schists, intensely deformed by several superimposed tectonic processes.

The foundation is laid on metaigneous rocks with a predominantly monzogranitic composition. It comprises deformed granite presenting subvertical foliation, slightly micaceous, with predominance of quartz and feldspar. The rock alteration results in layers of silty sand and sandy silt, with low clay content. Figure 1a illustrates the overview of the site area and Fig. 1b its division in sectors. The location of the rotary drilling borings is shown in the sectors with pile foundations in rock.

The subsoil investigation was carried out by percussion borings and rotary drilling (SPT/SM). Seismic profiles were made to characterize the bedrock and to estimate the mechanical properties of the foundation.

A complementary geophysical campaign was carried out. Rotary drillings identified the bedrock ranging from 0 to 12.7 m depth. In the first meters, the rock mass revealed poor quality, low recovery, highly weathered and intensively fractured.

Figure 2 shows a typical subsurface profile and rock section.

The complexity of the stratigraphy was verified with an alteration of the rock mass starting in the fractures, resulting in lateral contacts between soil and rock and the occurrence of numerous boulders in the soil mass.

With the samples taken from the rock, laboratory tests were carried out to obtain the index properties (absorption, porosity, natural and saturated specific weight) and mechanical properties (uniaxial compressive strength of the intact rock).



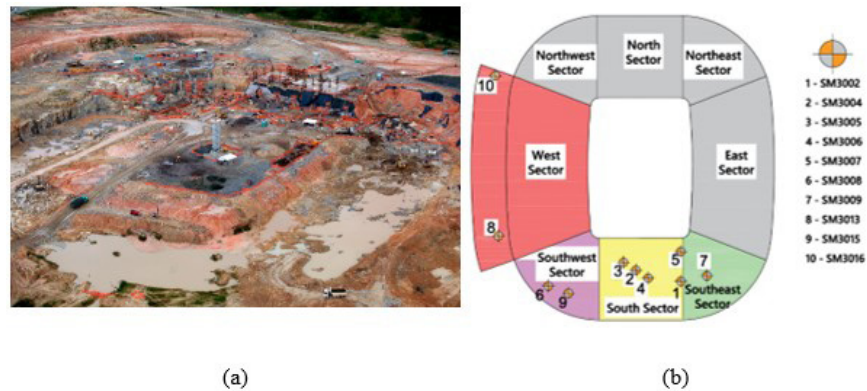


Figure 1. (a) site view; (b) area subdivided in different sectors.

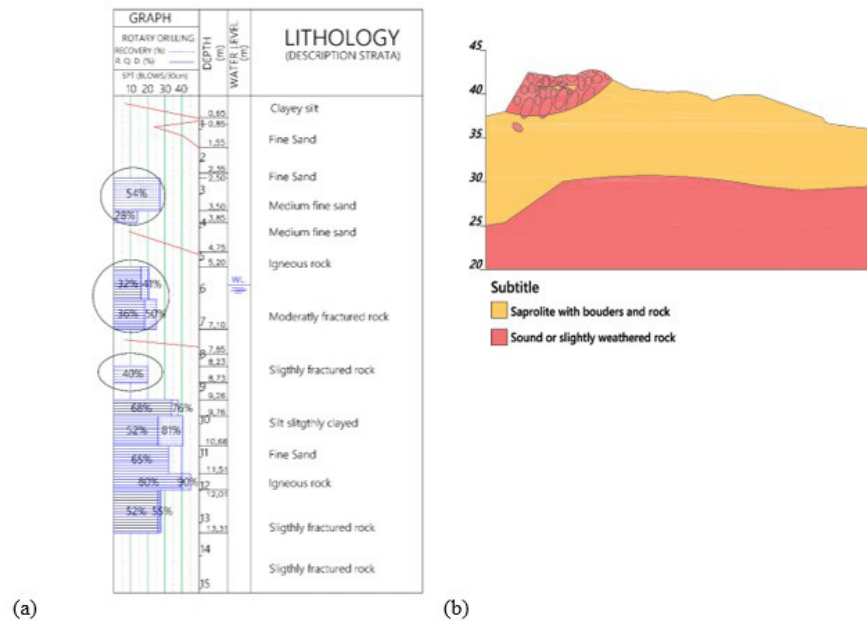


Figure 2. (a) percussion boring and rotary drilling; (b) typical section- Southeast Sector.

The strong presence of boulders makes the investigation analyses much more difficult.

Some samples obtained from rotary drilling underwent petrographic analysis and uniaxial compressive strength tests that varied over a wide range [12.27-121.39 MPa], indicating the need to observe other features of the rock mass. This range is investigated later for the different sectors. The observed behavior did not indicate mechanical parameters improving with depth.

Figure 3 illustrates the rocky features in the Southeast Sector, with major weathering and variable aspect, intense heterogeneity and highly fractured, with the presence of boulders and a very irregular surface.

Figure 4 illustrates the bedrock features in the South Sector. They are sub-vertical, of tectonic origin, with the occurrence of a sub-horizontal system, relief joints, forming a



Figure 3. Aspect of slope of Southeast Sector.

preferential percolation path, resulting in a very heterogeneous weathered profile. These features result in a spheroidal alteration system with boulders and a very fractured rock.

In the Southwest Sector the rock is composed of deformed granite, very foliated, with an irregular surface. The contact of soil and weathered rock is very heterogeneous and abrupt. The rock surface is very fractured, with the presence of saprolite and boulders.

An alluvial cover in the West Sector is overlaid by an existing landfill.

The geological structures are presented in the form of fractures and fractured zones, from which the alteration in the rock mass advances. A geological fault in an approximate ENE-WSW (east northeast, west southwest) direction was observed.

#### 4.2 Foundation characteristics and testing results

Two foundation solutions were adopted, depending on bedrock depth. Shallow foundations on rock were designed for bedrock to a depth of 5 m or less, and root piles for deeper depths. Figure 5a shows a general scheme of root piles embedded in rock and Figure 5b shows the foundation at shallow depths.

The estimated pile length was 4 m to 5 m in sound rock. The actual embedment length increased where unfavorable geological features occur due to severe weathering, revealed by rotary drilling or during pile installation.

A total of 99 dynamic load tests were analyzed by the CAPWAP program. Better quality signals were also selected and analyzed by DINEXP program. Table 5 summarizes the main pile design information and Table 6 includes the data obtained during ground investigation and installation of the tested piles, including the wide range of  $q_u$  values and statistical distributions for the different sectors.

Table 6 shows that the Southeast, Southwest and South Sectors showed a certain uniformity in the distribution of  $q_u$  of the intact rock, the  $RQD$  and pile length penetration in rock. In the West Sector, in addition to the lower average value of  $q_u$ , its variability also significantly exceeded the other sectors. However, pile penetration in rock presented the smallest mean value contrary to what might be expected. The lower penetration in rock was probably due to the higher  $RQD$  compared to the other sectors. This is an indication of the importance of geological features, other than  $q_u$  of the rock samples.

The recommendations from NBR 6122 (ABNT, 2019) were followed during piling installation. During the dynamic load test according to NBR 13208 (ABNT, 2007) the piles were subjected to twice the working load. In cases of imminent



Figure 4. South Sector with occurrence of boulders on its surface, zones of weathered and fractured rock.

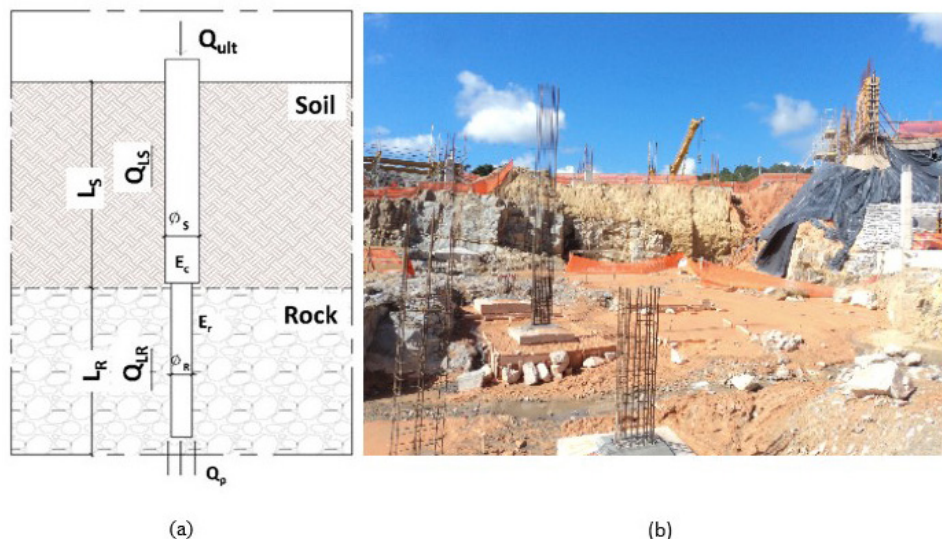
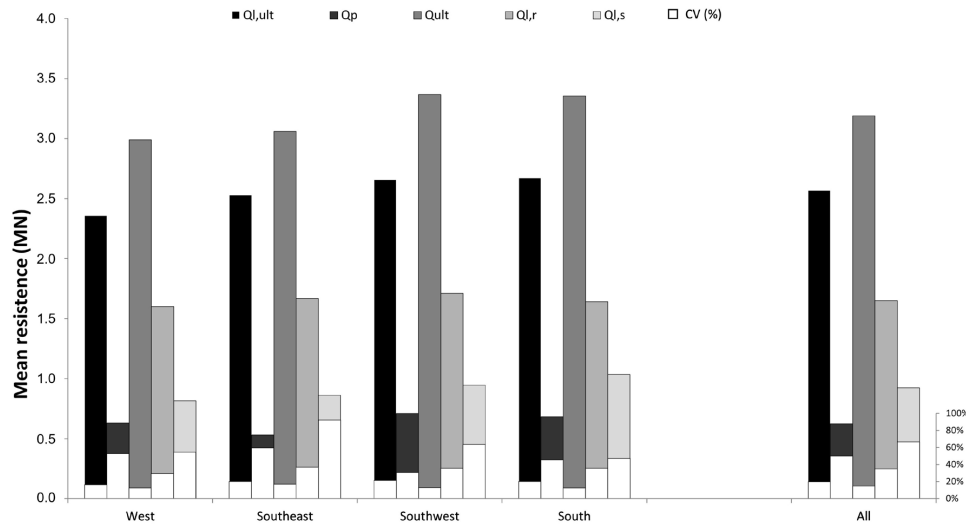


Figure 5. (a) general scheme of root piles embedded in rock; (b) foundation at shallow depths.



**Figure 6.** CAPWAP mobilized resistance (mean value) and its distribution in soil and rock.

**Table 5.** Characteristic of the root piles drilled in rock.

$\phi_s$ (mm)	$\phi_r$ (mm)	$L_s$ (m)	$L_r$ (m)	Design Load (kN)
310	310	1 to 12.2	3 to 8	1.100

**Table 6.** Statistical distribution of  $q_u$ ,  $RQD$ , pile length in soil and in rock.

Sector	Statistical Distribution	$q_u$ (MPa)	$RQD$ (%)	$L_s$ (m)	$L_r$ (m)
West	Mean	58.4	67%	5.4	4.7
	SD	38.4	25%	1.7	0.7
	CV	66%	38%	32%	15%
Southeast	Mean	97.5	42%	4.1	6.9
	SD	28.0	1.4%	1.9	1.3
	CV	29%	- *	46%	19%
Southwest	Mean	99.6	51%	4.6	5.3
	SD	24.2	14%	2.6	0.5
	CV	25%	28%	56%	9%
South	Mean	90.8	48%	8.3	5.5
	SD	19.3	19%	2.3	1
	CV	21%	39%	28%	18%

(\*) For the Southeast Sector only two samples were available, and the coefficient of variation could not be estimated. SD is the standard deviation and CV is the coefficient of variation.

structural damage or when unsatisfactory conditions were observed, loading was interrupted to ensure safety. The test results provided the maximum mobilized load for the blow of higher energy. The behavior of the tested piles was satisfactory. No failure or condition of significant settlements for the service load was reached.

According to Reese & O’Neill (1999), the toe resistance is mobilized for pile displacement of around 5% of the pile diameter in rock. Only 14 out of 99 tested piles had

displacements (DMX) of 8 mm-12 mm, which corresponds to between 2.5% and 3.9% of the pile diameter embedded in rock. Only 20% of the total mobilized capacity was resisted by the pile toe. The West Sector, with a broader variability, displayed greater displacements during the tests. Figure 6 presents the statistical distribution of CAPWAP results for the 99 piles.

The mobilized lateral shear observed in rock was tentatively compared to  $q_u$ . Unfortunately, a simple relationship between the mobilized lateral shear and  $q_u$ , or  $RQD$ , was not reached in the case in study, contrary to Juvêncio et al. (2017) findings.

Juvêncio et al. (2017) presented an interpretation of dynamic tests on cast-in-place piles in gneissic rock in Rio de Janeiro. The authors obtained a relationship between  $q_u$  and the  $RQD$ . Values of mobilized lateral shear in dynamic tests of piles partially embedded in gneissic rock were compared to the  $q_u$  values derived from the  $RQD$  correlation. An expression of prediction of mobilized shear resistance was proposed by Juvêncio et al. (2017) for pile design in gneissic rock in Equation 21. Juvêncio et al. (2017) emphasized that since failure was not reached in the dynamic tests, the use of Equation 21 is a conservative approach.

$$\tau_{l,r} = \alpha (5 + 0.6RQD)^\beta \tau_{l,r, in MPa, RQD in \%} \quad (21)$$

Juvêncio et al. (2017) suggested the values of 0.2 and 0.3 for the empirical adjustment parameters  $\alpha$  and  $\beta$ , very close to Horvath (1978). They also found that in the Rio de Janeiro gneiss, which is only slightly fractured,  $RQD$  has a direct relationship with weathering.

In fact, the results of the statistical distribution of  $q_u$  and  $RQD$  in Table 6 did not indicate a direct relation, especially in the West Sector. The rock mass in the present case is formed mainly by granites of different compositions, gneiss and schists, with marked weathering and intense fragmentation.



Those were probably the reason for the difficulty to establish a correlation in the present case. Dynamic test interpretation in terms of total mobilized resistance was the alternative in the following sections.

The lowest mobilized total resistance in Figure 6 was found in the West Sector, with the lower mean and most variable  $q_u$ . All sectors presented the same approximate percentage (nearly 20%) of load mobilization at the pile toe. The largest contribution of the mobilized capacity was the 50% lateral resistance in rock. However, the lateral resistance mobilized in soil of nearly 28% should not be disregarded. A significant value of lateral resistance in soil occurred also in Sectors West and Southwest, with a pile length in soil comparable to that in rock.

In relation to the coefficient of variation, the lowest values were observed for the total mobilized resistance,  $Q_{ult}$ . A wide dispersion was found for the tip resistance  $Q_p$ . Regarding lateral resistance, it is found that, although the main contribution is due to rock, its variability was much smaller than that in soil. Lateral mobilized resistance in soil ( $Q_{l,s}$ ) presented a mean coefficient of variation of 67%, due to the high variability in soil profile. For the lateral resistance in the rock ( $Q_{l,r}$ ) the coefficient of variation was much lower, close to 35%. Experience shows that the variability of tip resistance in soil mass is reasonably higher than that occurring in the shaft. The same was observed in the present analyses in the mobilized resistance in rock.

Another set of analyses were carried out with DINEXP program. The distribution of lateral resistances in rock and in soil and the corresponding statistical distribution were obtained and compared to CAPWAP analyses. Figure 7 shows the statistical results.

Unlike CAPWAP results, the Southeast Sector presented the lowest total mobilized resistance in DINEXP analyses. As the CAPWAP program was applied to 99 tests and DINEXP to 46, the difference in the mean value, close to 7%, is of no significance, especially when the uniqueness of CAPWAP results is taken into account (e.g. Danziger et al., (1996)).

The statistical distribution of mobilized resistances obtained by CAPWAP in a group of 99 tested piles is very close to the DINEXP in a group of 46 piles. The smallest coefficients of variation of DINEXP analyses were also found in the total mobilized resistance,  $Q_{ult}$  in Figure 7. A high dispersion range was found in the mobilized toe resistance,  $Q_p$ , with a coefficient of variation of 62%, much higher than that of the CAPWAP, but consistent with the experience with static and dynamic tests. The lateral resistance transferred to the soil ( $Q_{l,s}$ ) in the analyses with DINEXP also indicated low uniformity, with a coefficient of variation of 50%. For the lateral resistance mobilized in rock ( $Q_{l,r}$ ) the coefficient of variation was much lower, 33%, very similar to CAPWAP results.

Both programs indicated that lateral capacity in soil should not be disregarded.

Juvêncio et al. (2017) also observed a significant contribution of the residual soil overlying the rock in the lateral capacity of the 30 dynamic tests of partially embedded piles in a granitic rock with a gradual weathered degree of alteration.

The measured and estimated force and/or velocity at the pile top indicated a very good match with the application of both CAPWAP and DINEXP program. The results confirmed the literature indications: lateral capacity is the main contribution of resistance mobilization of piles partially embedded in

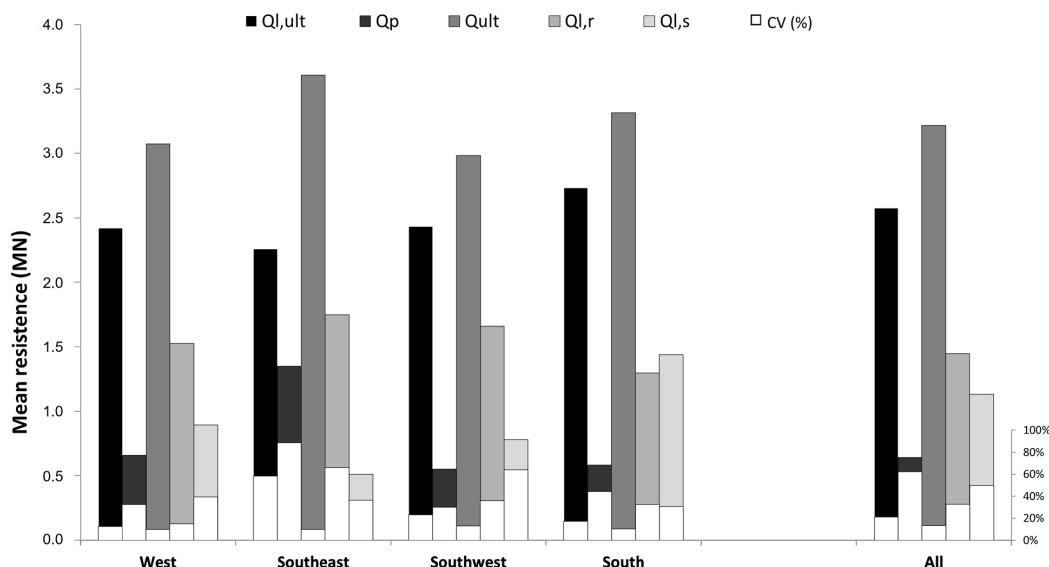


Figure 7. Mobilized mean resistance by DINEXP analysis and its distribution in soil and rock for 46 tested piles.



rock, reaching nearly 80% in the present case analyzed by CAPWAP and by DINEXP. The percentage of mobilization at the pile toe remained close to 20% for both programs. The contribution of each component of total resistance was 20%, 52% and 28% for mobilized tip resistance in rock, lateral resistance in rock and lateral resistance in soil for CAPWAP analyses and 20%, 45% and 35% for DINEXP.

Despite being disregarded in the literature, a significant contribution of lateral resistance in soil was found not only in this case in Recife but also in the database interpreted by Juvêncio et al. (2017) in Rio de Janeiro. The soil contribution, although smaller compared to lateral capacity in rock, reveals room for optimization in the design of deep foundations in root piles in rocks.

### 4.3 Bearing capacity estimation

The methods summarized in Section 2 were applied to the 99 tested piles. Some limitations of the methods are summarized below.

For Rosenberg & Journeaux (1976), the  $q_u$  was limited to  $5 \leq q_u / P_{atm} \leq 340$  and  $P_{atm} = 0.1 \text{ MPa}$ . As the  $q_u$  results exceeded this range, the upper limit  $q_u = 34 \text{ MPa}$  was applied in the estimations. For the methods of Horvath (1978), Meigh & Wolski (1979) and Zhang & Einstein (1998), the lateral capacity is related to the smallest value between  $q_u / P_{atm}$  and  $f_{ck} / P_{atm}$ . Once the  $q_u$  was higher than the characteristic compressive strength of the pile concrete,  $q_u > f_{ck}$ , the characteristic strength of the concrete was used.

The correlation by Rowe & Armitage (1987) was established for  $q_u \leq 30 \text{ MPa}$ , thus the upper limit of 30 MPa was used for all piles.

For the AASHTO (1996) method, lateral resistance is given by the smallest value between  $q_u / P_{atm}$  and  $f_{ck} / P_{atm}$ , but here a reduction factor based on the  $RQD$  is used. For Cabral & Antunes (2000) and Poulos & Davis (1980) methods, the  $q_u$  defined in each sector for each pile was maintained. The method proposed by España (2011) uses coefficients related

to the rock type, degree of weathering of the rock mass and discontinuity spacings to determine the allowable stress ( $P_{v,adm}$ ).

In the application of the Xu et al. (2020) method, the  $q_u$  of the intact rock was used, associated to the  $RQD$  and the influence of the discontinuity of the rock mass.

The load capacity of the tested piles was estimated by the selected methods and compared to the mobilized resistance obtained by the DINEXP program.

The comparison between the estimated and the mobilized capacity from the dynamic load testing was established for the lateral resistance in soil, lateral resistance in rock, toe resistance in rock and total capacity.

The estimation of lateral capacity in soil ( $Q_{l,s}$ ) was predicted and compared to the mobilized capacity in Table 7 in terms of its statistical distribution and in Figure 8 for each of the 46 tested piles analyzed by DINEXP program.

Figure 8 indicates the ratio estimated to mobilized lateral capacity in soil between 2.7 and 5.5, revealing much higher estimated capacities than the mobilized ones. Similar results were found by Juvêncio et al. (2017).

The estimation of lateral capacity in rock ( $Q_{l,r}$ ) was predicted by Rosenberg & Journeaux (1976), Horvath (1978), Meigh & Wolski (1979), Poulos & Davis (1980), Rowe & Armitage (1987), Cabral & Antunes (2000), AASHTO (1996), Zhang & Einstein (1998), España (2011) and Xu et al. (2020). The estimated and mobilized capacities in rock are presented in Table 8 and in Figure 9 the values are indicated for each of the 46 tested piles analyzed by the DINEXP program.

Similar results were found by Juvêncio et al. (2017) who justified that failure values were not reached in the dynamic tests due mainly to the limited delivered energy. Another reason that contributed to the low mobilized values compared to predicted failure values is that the design methods were conceived for sedimentary rocks, with failure values more easily reached in load testing (Juvêncio et al., 2017).

The toe capacity in rock ( $Q_p$ ) was predicted by Poulos & Davis (1980), Rowe & Armitage (1984), Cabral & Antunes

**Table 7.** Statistical distribution of mobilized and estimated lateral capacity of soil,  $Q_{l,s}$  (kN).

Statistical Distribution	Sector	Aoki & Velloso (1975)	Décourt (1996)	Cabral (1986)	Mobilized Resistance
Mean	West	221.2	492.8	312.3	163.4
SD		76.8	177.6	146.8	83.6
CV		35%	36%	47%	51%
Mean	Southeast	137.2	439.7	383.7	51
SD		75.8	240.5	230.1	18.6
CV		55%	55%	60%	36%
Mean	Southwest	236.7	478.5	254.9	83.3
SD		129.8	285.9	213.2	74.5
CV		55%	60%	84%	89%
Mean	South	479.9	921.4	610.6	143.8
SD		318.3	360	408.2	44.1
CV		66%	39%	67%	31%

**Table 8.** Statistical distribution of mobilized and estimated lateral resistance of pile in rock,  $Q_{l,r}$  (kN).

Statistical Distribution	Sector	Rosenberg & Journeaux (1976)	Horvath (1978)	Meigh & Wolski (1979)	Poulos & Davis (1980)	Rowe & Armitage (1987)	AASHTO (1996)	Zhang & Einstein (1998)	Cabral & Antunes (2000)	España (2011)	Xu et al. (2020)	Mobilized Capacity
Mean	West	10586.00	5254.3	6238.8	6250.4	11583.3	387.5	8406.9	702.4	1697.9	5955.2	1497.0
SD		2322.7	1152.8	1368.8	1371.4	2541.5	85	1844.5	154.1	523.7	1773.8	225.2
CV		22%	22%	22%	22%	22%	22%	22%	22%	31%	30%	15%
Mean	Southeast	16970.9	8423.4	10001.7	10020.4	18569.7	621.3	13477.4	1126.0	3309.4	11303.6	1713.5
SD		3352.8	1664.2	1976.0	1979.7	3668.7	122.7	2662.7	222.5	653.8	2233.2	1130.2
CV		20%	20%	20%	20%	20%	20%	20%	20%	20%	20%	66%
Mean	Southwest	12054.5	5983.20	7104.3	7117.5	13190.2	441.3	9573.1	799.8	2815.4	9337.2	1626.0
SD		1945.4	965.6	1146.5	1148.7	2128.7	71.2	1544.9	129.1	606.8	1920.7	458.9
CV		16%	16%	16%	16%	16%	16%	16%	16%	22%	21%	28%
Mean	South	12007.3	5959.8	7076.4	7089.7	13138.6	439.6	9535.6	796.7	2210.3	7841.3	1270.2
SD		2498.20	1240.0	1472.3	1475.0	2733.5	91.5	1983.9	165.7	845.2	2677.0	412.4
CV		21%	21%	21%	21%	21%	21%	21%	21%	38%	34%	32%

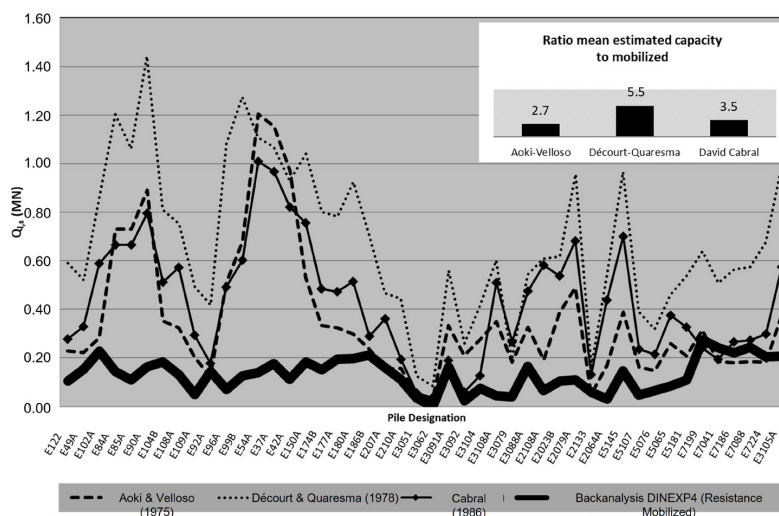


**Figure 8.** Estimated and mobilized lateral capacity in soil for each pile.

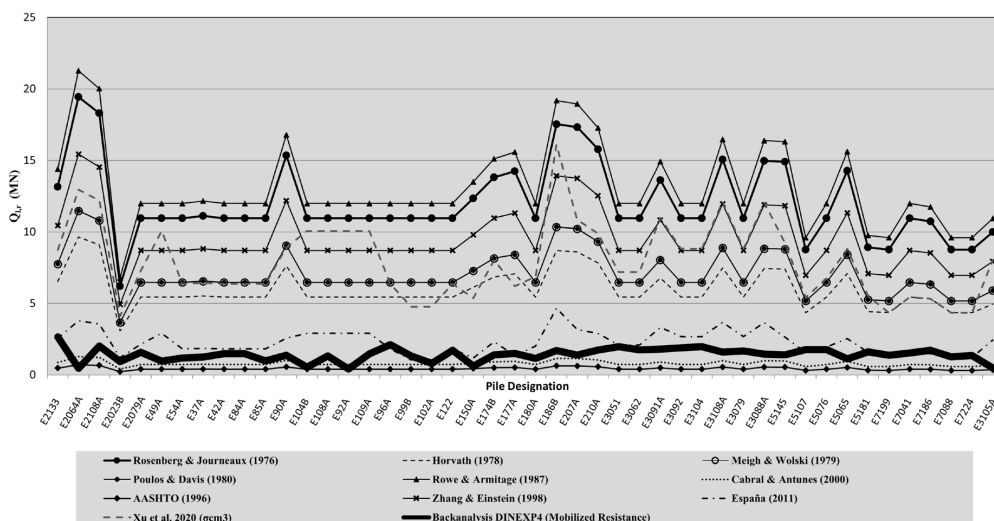


**Figure 9.** Estimated lateral capacity and mobilized capacity in rock.

(2000), AASHTO (1996) and España (2011). The estimated and mobilized toe capacity are presented in Table 9 and in Figure 10 for each tested pile analyzed by DINEXP program.

The estimated and the mobilized total capacity ( $Q_{ult}$ ) are presented in Table 10 and in Figure 11 for the 46 tested piles analyzed by the DINEXP program. Only the lateral resistance in rock ( $Q_{l,r}$ ) and the toe resistance in rock ( $Q_p$ ) were considered in the estimations. Results from the loading tests included the whole mobilized capacity in rock and the lateral resistance in soil ( $Q_{l,s}$ ).

Four out of ten methods applied do not consider the toe resistance contribution: Rosenberg & Journeaux (1976), Horvath (1978), Meigh & Wolski (1979) and Xu et al. (2020). Even with this conservative approach, the application of all

these design methods resulted in estimated capacity much greater than the mobilized resistance obtained in the tests.

Figure 11 shows the great variations found. It seems clear that the methods of Rosenberg & Journeaux (1976), Rowe & Armitage (1987) and Zhang & Einstein (1998) presented very high estimates of total bearing capacity compared to the other methods. The application of the methods from España (2011), Cabral & Antunes (2000) and AASHTO (1996) resulted in estimates with closer agreement to the mobilized load in the tests.

#### 4.4 Static load testing

The static load testing did not characterize the soil failure. Some extrapolation methods were adopted to obtain

**Table 9.** Statistical distribution of mobilized and estimated toe resistance in rock,  $Q_p$  (kN).

Statistical Distribution	Sector	Poulos & Davis (1980)	Rowe & Armitage (1987)	AASHTO (1996)	Zhang & Einstein (1998)	Cabral & Antunes (2000)	España (2011)	Mobilized Resistance
Mean	West	603.5	2263.2	72.5	1012.1	322.1	539	643.8
SD		-	-	-	-	-	69.3	209.8
CV		-	-	-	-	-	13%	33%
Mean	Southeast	603.5	2263.2	72.5	1012.1	322.1	662.7	1323.2
SD		-	-	-	-	-	-	1174.2
CV		-	-	-	-	-	-	89%
Mean	Southwest	603.5	2263.2	72.5	1012.1	322.1	790.1	537.7
SD		-	-	-	-	-	79.2	314.3
CV		-	-	-	-	-	10%	58%
Mean	South	603.5	2263.2	72.5	1012.1	322.1	626.4	570.5
SD		-	-	-	-	-	205.6	241.9
CV		-	-	-	-	-	33%	42%

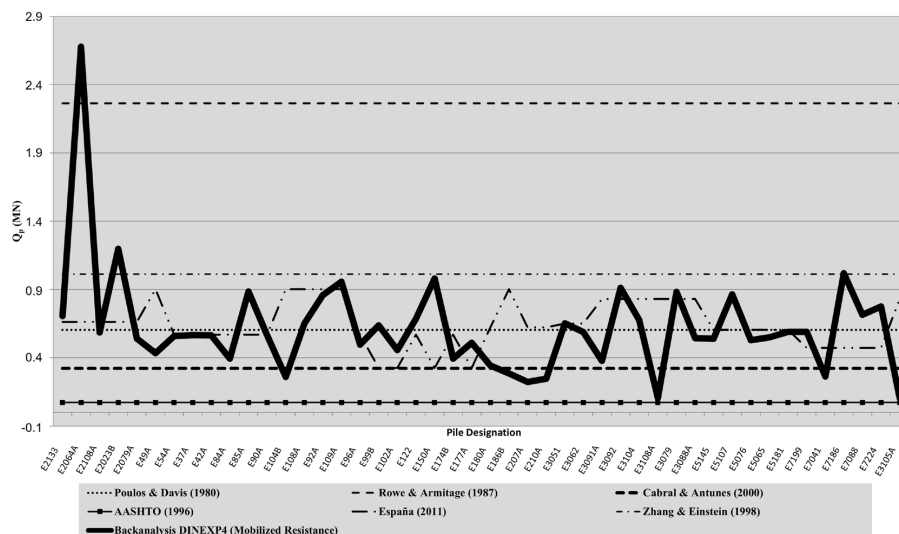


**Figure 10.** Estimated and mobilized toe capacity in rock.

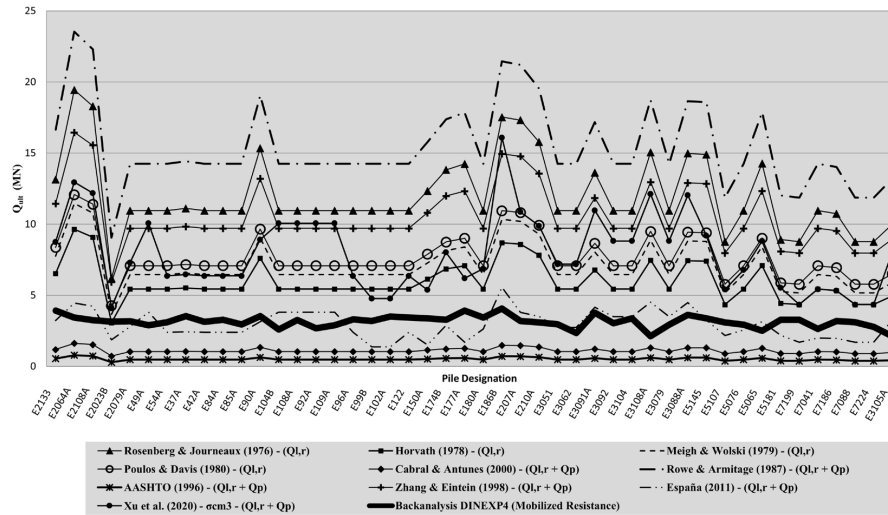


Figure 11. Estimated and mobilized total bearing capacity.

Table 10. Statistical distribution of mobilized and estimated total bearing capacity,  $Q_{ult}$  (kN).

Statistical Distribution	Sector	Rosenberg & Journeaux (1976)	Horvath (1978)	Meigh & Wolski (1979)	Poulos & Davis (1980)	Rowe & Armitage (1987)	AASHTO (1996)	Zhang & Einstein (1998)	Cabral & Antunes (2000)	España (2011)	Xu et al. (2020)	Mobilized Resistance
Mean	West	10586.0	5254.3	6238.8	6853.9	13846.4	460	9419.0	1024.5	2236.9	5955.2	3016.2
SD		2322.7	1152.8	1368.8	1371.4	2541.5	85	1844.5	154.1	576	1773.8	294.1
CV		22%	22%	22%	20%	18%	18%	20%	15%	26%	30%	10%
Mean	Southeast	16970.9	8423.4	10001.7	10623.9	20832.9	693.8	14489.6	1448.1	3972.1	11303.6	3537.3
SD		3352.8	1664.2	1976.0	1979.7	3668.7	122.7	2662.7	222.5	653.8	2233.2	345.1
CV		20%	20%	20%	19%	18%	18%	18%	15%	16%	20%	10%
Mean	Southwest	12054.5	5983.2	7104.3	7721.1	15453.4	513.8	10585.2	1121.9	3605.6	9401.5	2926.7
SD		2129.7	1057.1	1255.1	1257.5	2330.3	78	1691.3	141.3	520.2	4168.6	666.6
CV		18%	18%	18%	16%	15%	15%	16%	13%	14%	44%	23%
Mean	South	12007.3	5959.8	7076.4	7693.2	15401.7	512.1	10547.7	1118.8	2836.7	7841.3	3250.8
SD		2498.2	1240.0	1472.3	1475.0	2733.5	91.5	1983.9	165.7	1005.0	2677.0	337.1
CV		21%	21%	21%	19%	18%	18%	19%	15%	35%	34%	10%

a conventional failure load: Terzaghi (1943), Van Der Veen (1953), Chin (1970, 1971), Davisson (1972), Décourt (1996) and ABNT (2019). Due to the lack of an experimental value for pile concrete modulus, the value of 25 GPa was considered in the interpretation of the pile elastic shortening by Davisson (1972) and ABNT (2019) methods.

For each pile two extrapolated conventional failure loads were indicated in Table 11. The column designated by S provides the results extrapolated from the slow maintained loading and the column designated by Q shows the results extrapolated from the quick maintained load.

Except for pile E184, the quick tests indicate a higher failure load compared to the slow maintained tests, as expected (Lopes et al., 2021).

Only Pile E122 was submitted to both dynamic and static testing, the former three (3) months before the static test. The conventional failure load from the static tests shown in Table 11 were very similar, except for Chin (1970, 1971)

and Décourt (1996) methods. Excluding those two methods, the mean conventional failure load for the slow maintained test for pile E 122 is 3890 kN and the mobilized resistance by CAPWAP analysis is 3432 kN, the former being 12% greater than the latter. If the quick maintained static load testing is considered, the convention failure load is 4396 kN, a value 28% greater than the CAPWAP result.

In Table 12 the mobilized resistance from the CAPWAP of a pile very close to that of the static tested piles are compared. The piles with compared results have the same penetration in rock. The CAPWAP mobilized resistance of pile E7041 is compared to the conventional failure load of rapid test on pile E 7043. Pile E5065 is compared to E5043, E5107 to E5103 and E 186B to E184. Only the pile E122 is compared to itself. All the conventional failure loads in Table 12 correspond to the mean value considering the results from the cited methods, except Chin (1970, 1971) and Décourt (1996). The choice of the rapid maintained test



**Table 11.** Extrapolated conventional failure loads for the slow and quick maintained static loading tests interpreted for the 5 tested piles.

Method	E7043 (KN)		E5043 (KN)		E5103 (KN)		E184 (KN)		E122 (KN)	
	S	Q	S	Q	S	Q	S	Q	S	Q
Terzaghi (1943)	6400	7030	3920	5100	3350	3416	5200	2948	3900	4390
Van Der Veen (1953)	6664	7350	4410	5880	3430	3430	*	2940	3920	4410
Chin (1970, 1971)	10000	12500	10000	10000	5000	10000	10000	5000	10000	10000
Davisson (1972)	6540	7248	3628	5200	3200	3377	5250	2940	3855	4385
Décourt (1996)	9716	11681	8400	8529	5554	5858	11947	4537	9048	6818
ABNT (2019)	6598	7300	2499	5390	3300	3403	5255	2948	3890	4400

(\*) Inconsistent extrapolated value.

**Table 12.** Mobilized resistance compared to conventional failure load from static test.

Pile	E7041	E7043	E5065	E5043	E5107	E5103	E186B	E184	E122	E122
	$Q_{ult}$ (mobilized)	$Q_{ult,mean}$ (extrapolated)	$Q_{ult}$ (mobilized)	$Q_{ult,mean}$ (extrapolated)	$Q_{ult}$ (mobilized)	$Q_{ult,mean}$ (extrapolated)	$Q_{ult}$ (mobilized)	$Q_{ult,mean}$ (extrapolated)	$Q_{ult}$ (mobilized)	$Q_{ult,mean}$ (extrapolated)
Mobilized and Conventional Failure Load (KN)	2643	7232	2500	5392	3090	3407	4069	2948	3432	4396
Ratio Conventional Failure load to Mobilized Load (%)	2.7		2.2		1.1		0.72		1.3	

instead of the slow maintained test in Table 12 is a result of the higher load reached in the test, allowing a much reliable interpretation of the extrapolated conventional failure load.

Comparing the results from pile E122, the only submitted to both dynamic and static loading test, to the mean value from the remaining tests (except E184), it can be observed the following: a value of the ratio conventional failure load to mobilized resistance of 1.3 for pile E122 and 2 for the remaining piles.

As long as pile E122 presented a conventional failure load in the quick static load test 1.13 times the value obtained in the slow maintained load, the following can be inferred: the expected conventional static failure load in a slow maintained load is close to 1.2 to 1.8 times the mobilized values obtained in the dynamic test in this case study. The results of the static load testing reassure room for optimization in the design of deep foundations in root piles in rocks.

## 5. Conclusions

All tested piles presented a satisfactory mobilized capacity in the dynamic load tests.

The CAPWAP analysis applied to 99 piles produced similar results as the equivalent program DINEXP applied to 46 out of the 99 tested piles, presenting a good accuracy, with similar resistance distribution at toe, lateral resistance in soil and lateral resistance in rock.

The mobilized resistance from shaft penetration in soil was between 28% and 35% of the total mobilized resistance. However, many design methods do not consider this component in their estimations.

Despite the inclusion of a more complete characterization of the rock mass, España (2011) and Xu et al. (2020) design methods did not produce a predictive capacity closer to that mobilized in the tests. Yet España (2011) presented results that can be considered in an analysis in which the rock characterization is well performed. The other methods including a much simpler rock characterization, such as Cabral & Antunes (2000) and AASHTO (1996), resulted in an estimation closer to the mobilized resistance for lateral capacity in rock.

The bearing capacity design methods of an empirical nature indicated results against safety for the piles partially penetrating rocks in this case study. The methods from

Rosenberg & Journeaux (1976), Rowe & Armitage (1987) and Zhang & Einstein (1998) should not be applied to similar situations as that presented.

An alternative suggestion for design proposals for piles in similar conditions to those analyzed in the paper is a composition involving the Aoki & Velloso (1975) method for shaft penetration in soil and España (2011), Cabral & Antunes (2000) or AASHTO (1996) for the shaft penetration in rock.

The expected conventional static failure load in a slow maintained load is close to 1.2 to 1.8 times the mobilized values obtained in the dynamic tests. The static load testing reaffirms the conclusions obtained in this case study.

## Acknowledgements

To the REAGEO Project promoted by the National Institute for the Recovery of Slopes and Plains and the company Geomec for providing the dynamic loading test signals.

## Declaration of interest

There are no conflicting interests.

## Author's contributions

Marília Dantas da Silva: data curation, conceptualization, methodology, validation, writing - original draft. Roberto Quental Coutinho: validation, supervision, writing - reviewing and editing. Bernadete Ragoni Danziger: data curation, validation, supervision, writing - reviewing and editing.

## List of symbols

$A_t$	pile toe section
$d_f$	embedded factor to the tip resistance
$F_2$	factor expressing the influence of installation and scale effects
$f_{ck}$	concrete characteristic strength in compression
$k$	CPT x SPT correlation value depending on soil type
$L_r$	pile length in rock
$\bar{N}$	factor related to the quality of the rock mass
$\bar{N}$	average $N_{60}$ value for the whole shaft penetration in soil
$n$	correction factor that considers the rock alteration degree and the presence of small fractures in rock mass
$N_L$	average $N_{60}$ value for a given soil layer with a $\Delta L$ penetration
$N_{ms}$	coefficient that depends on rock type and quality
$P_{v,adm}$	allowable stress by method proposed by España (2011) uses coefficients related to the rock type, degree

$p_0$	reference stress (1 MPA)
$Q_{l,r}$	lateral resistance in rock
$Q_{l,s}$	lateral resistance in soil
$Q_p$	toe resistance in rock
$Q_{p,r}$	resistance at pile tip
$q_{p,r}$	rock unit tip resistance
$q_u$	uniaxial compressive strength of the intact rock
$Q_{ult}$	mobilized total capacity
$S$	spacing (in meters) between discontinuities
$U$	perimeter of the pile shaft section
$\alpha$	CPT x SPT correlation values depending on soil type
$\alpha$	factor related to the quality of the rock mass
$\alpha_1, \alpha_2, \alpha_3$	dimensionless parameters depending on rock type, alteration degree and discontinuities spacing, respectively
$\beta$	empirical parameter
$\beta'$	coefficient given by Décourt (1996)
$\beta_0, \beta_1$	coefficients given by Cabral (1986)
$\Delta L$	penetration in each soil layer
$\delta_0$	elastic displacement in mm
$\rho$	empirical parameter
$\sigma_{cm3}$	resistance compressive of rock mass using RQD and considering the influence of discontinuities given by Xu et al. (2020)
$\sigma_t$	is the rock tensile strength
$\tau_{l,r}$	unit shear resistance
$\tau_{l,s}$	shear soil resistance
$\tau_{max}$	the shear resistance in rock
$\phi_r$	the pile diameter in rock
$\phi_s$	he diameter of pile penetrated in soil

## References

- AASHTO. (1996). *Standard Specifications for Highway Bridges*. American Association of State Highway and Transportation Officials, Washington, D.C.
- ABNT NBR 13208. (2007). *Dynamic Testing of Piles – Test Method*. ABNT – Associação Brasileira de Normas Técnicas, Rio de Janeiro, RJ (in Portuguese).
- ABNT NBR 6122. (2019). *Design and execution of foundations*. ABNT – Associação Brasileira de Normas Técnicas, Rio de Janeiro, RJ (in Portuguese).
- Aoki, N., & Velloso, D.A. (1975). An approximate method to estimate the bearing capacity of piles. In *Proceedings of the 5th Pan. Conference on Soil Mechanics and Foundations: Vol. 5* (pp. 367-374). Buenos Aires.
- Cabral, D.A. (1986). The use of root piles as foundation of normal works. In *Proceedings of the Brazilian Conference on Soil Mechanics and Foundation Engineering: Vol. 6* (pp. 71-82). Porto Alegre. (in Portuguese).
- Cabral, D.A., & Antunes, W.R. (2000). A suggestion for bearing capacity estimation of piles embedded in rock.

- In *Proceedings of the Conference on Geot. Eng. Special Found: Vol. 4*. São Paulo. (in Portuguese).
- Chin, F.K. (1970). Discussion: Pile tests. Arkansas River Project. *Journal of the Soil Mechanics and Foundations Division*, 97(SM7), 930-932.
- Chin, F.K. (1971). Discussion of pile test. Arkansas River Project. *Journal for Soil Mechanics and Foundation Engineering*, 97(SM6), 930-932.
- Costa, A.M. (1988). *DINEXP Program developed*. CENPES/Petrobras.
- Danziger, B.R. (1991). *Dynamic Analysis of Driven Piles* [Unpublished doctoral dissertation]. Coppe/UFRJ.
- Danziger, B.R., Costa, A.M., Lopes, F.R., & Pacheco, M.P. (1996). A discussion on the uniqueness of CAPWAP-type analyses. In *Proceedings of the 5th International Congress on the Application of Stress-Wave Theory to Piles: Vol. 1* (pp. 394-408). Miami.
- Davissson, M.T. (1972). *High capacity piles* (Proceedings, Lecture Series. Innovations in Foundation Construction, pp. 52). ASCE, Illinois.
- Décourt, L. (1996). Analysis of deep foundations: piles. In Hachich. *Foundations: theory and practice* (pp. 265-301) Editora Pini Ltda. (in Portuguese).
- Décourt, L., & Quaresma, A. (1978). Pile load capacity from SPT values. In *Proceedings of the VI Brazilian Conference Cobramseg: Vol. 1* (pp. 45-53). Rio de Janeiro (in Portuguese).
- España. (2011). *Guía de cimentaciones en obras de carretera*. Ministerio de Fomento, Centro de Publicaciones.
- Goble, G.G., Rauche, F., & Likins, G.E. (1980). The Analise of Pile Driving – A State of the Art Report. In *Proceedings of the 2nd International Conference on the Application of Stress – Wave Theory to Piles* (pp. 131-161). Stockholm.
- Goble. (1986). *Notes on the course of Application of Stress Wave in Driven Piles*. PUC. (in Portuguese).
- Goodman, R.E. (1989). *Introduction to Rock Mechanics*. John Wiley & Sons.
- Horvath, R. (1978). *Field load test data on concrete-to-rock bond strength for drilled pier foundations* (Publication 78-07). University of Toronto.
- Juvêncio, E.L., Lopes, F.R., & Nunes, A.L.L.S. (2017). An Evaluation of the Shaft Resistance of Piles Embedded in Gneissic Rock. *Soils and Rocks, São Paulo*, 40(1), 61-74.
- Lopes, F.R., Santa Maria, P.E.L., Danziger, F.A.B., Martins, I.S.M., & Tassi, M.C. (2021). A proposal for static load tests on piles: the Equilibrium Method. *Soils and Rocks, São Paulo*, 44, 1-10.
- Meigh, A.C., & Wolski, W. (1979). Design parameters for weak rock. In *Proceedings of the 7th European Conference on Soil Mechanics and Foundation Engineering: Vol. 5* (pp. 59-79). London. British Geotechnical Society, Brighton.
- Poulos, H.G., & Davis, E.H. (1980). *Pile Foundation Analysis and Design*. John Wiley & Sons.
- Reese, L.C., & O'Neill, M.W. (1999). *Drilled Shafts: construction procedures and design methods* (Report FHWA-IF-99-025). Federal Highway Administration.
- Rosenberg, P., & Journeaux, N. (1976). Friction and end bearing tests on bed rock for high-capacity socket design. *Canadian Geotechnical Journal*, 13(3), 324-333.
- Rowe, R.K., & Armitage, H.H. (1984). *The design of piles socketed into weak rock* (Report GEOT-11-84). University of Western Ontario.
- Rowe, R.K., & Armitage, H.H. (1987). A design method for drilled piers in soft rock. *Canadian Geotechnical Journal*, 24(1), 126-142.
- Seidel, J.P., & Collingwood, B. (2001). A new socket roughness factor for prediction of rock socket shaft resistance. *Canadian Geotechnical Journal*, 38, 138-153.
- Simons, H.A., & Randolph, M.F. (1985). A new approach to one dimensional pile driving analysis. In *Proceedings of the 5th International Congress on Numerical Methods in Geomechanics*. Nagoya.
- Smith, E.A.L. (1960). Pile driving analysis by the Wave Equation. *Journal of the Soil Mechanics and Foundations Division*, 127(I), 1145-1193.
- Terzaghi, K. (1943). *Theoretical soil mechanics*. John Wiley & Sons.
- Van Der Veen, C. (1953). The bearing capacity of a pile. In *International of the 3rd Conference of Soil Mechanics and Foundation Engineering: Vol. 2* (pp. 84-90). Zurich: ICOSOMEF.
- Xu, J., Gong, W., Gamage, R.P., Zhang, Q., & Dai, G. (2020). A new method for predicting the ultimate shaft resistance of rock-socketed drilled shafts. *Proceedings of the Institution of Civil Engineers–Geotechnical Engineering*, 173(2), 169-186. <http://dx.doi.org/10.1680/jgeen.18.00221>.
- Zhang, L., & Einstein, H.H. (1998). End bearing capacity of drilled shafts in rock. *Journal of Geotechnical and Geoenvironmental Engineering*, 124(7), 574-584.